European Journal of Mechanics A/Solids 61 (2017) 122–133

Contents lists available at ScienceDirect

European Journal of Mechanics A/Solids

journal homepage: www.elsevier.com/locate/ejmsol

An edge dislocation near a nanosized circular inhomogeneity with interface slip and diffusion

Xu Wang [a], Cuiying Wang [a], Peter Schiavone [b, *]

[a] School of Mechanical and Power Engineering, East China University of Science and Technology, 130 Meilong Road, Shanghai 200237, China
[b] Department of Mechanical Engineering, University of Alberta, 10-203 Donadeo Innovation Centre for Engineering, Edmonton, Alberta T6G 1H9, Canada

ARTICLE INFO

Article history:
Received 25 April 2016
Received in revised form
23 August 2016
Accepted 7 September 2016
Available online 9 September 2016

Keywords:
Inhomogeneity
Edge dislocation
Surface elasticity
Rate-dependent slip
Diffusion
Relaxation time
Image force
Analytical continuation
State-space equation

ABSTRACT

We study the transient elastic field induced by an edge dislocation near a nanosized circular elastic inhomogeneity in which the effects of interface slip and diffusion are incorporated into the model of deformation. Separate Gurtin-Murdoch surface elasticities are specified on the surface of the inhomogeneity and on the adjoining surface of the surrounding matrix. In addition, rate-dependent interface slip and diffusion are assumed to occur concurrently on the inhomogeneity-matrix interface. The ensuing interaction problem is solved using a simple yet effective method based on analytic continuation and a convenient decomposition of the proposed solution. In particular, our method allows us to circumvent the second-order tangential derivative taken with respect to the interfacial normal stress, typically a source of additional complication and often an obstacle to the solution of such problems. The original problem is reduced to two coupled linear algebraic equations and a number of mutually independent sets of state-space equations, the general solutions of which can be obtained by solving the associated generalized eigenvalue problem. The image force acting on the edge dislocation is derived using the Peach-Koehler formula. Corresponding stress and displacement fields as well as the image force are found to be dependent on four size-dependent dimensionless parameters (arising from the surface elasticities) and on two size-dependent parameters (having the dimension of time) arising from the incorporation of interface slip and diffusion and they evolve with an infinite number of size-dependent relaxation times.

1. Introduction

The interaction between dislocations and second-phase inhomogeneities plays an important role in the creep behaviors of composites and polycrystalline solids (Srolovitz et al., 1984; Wei et al., 2008). When the dimensions of the inhomogeneity lie in the nanometer range, the following two main factors take on major significance in the modelling and analysis of nanostructured solids. The first concerns the contribution of surface/interface stresses, tension and energies (Sharma and Ganti, 2004). These surface effects can be incorporated into continuum-based models by using the surface/interface model of Gurtin and Murdoch (Gurtin and Murdoch, 1975, 1978; Gurtin et al., 1998). The Gurtin-Murdoch surface elasticity model is equivalent to the assumption of a thin and stiff two-dimensional membrane perfectly bonded to the surface of a three-dimensional bulk (Steigmann and Ogden, 1997; Chen et al., 2007; Antipov and Schiavone, 2011; Markenscoff and Dundurs, 2014). The second major factor requiring consideration in nanostructured solids is rate-dependent interface slip and diffusion (Wei et al., 2008). Interface slip can be seen as local diffusion on a length scale comparable to the size of the asperities of the interface (Raj and Ashby, 1971), whilst long range interface diffusion is driven by the gradients of the chemical potential on the interface (Herring, 1950). Interface slip and diffusion contribute to room temperature plastic deformations in nanocrystalline materials. The co-existence of interface slip and diffusion makes the ensuing analysis extremely challenging even in the absence of surface elasticity (Wang and Pan, 2010, 2011).

This paper endeavors to consider the coupled effects of surface elasticity, interface slip, interface diffusion and dislocation emission/absorption on the transient deformations of nanostructured materials. More specifically, we investigate the elastic interaction between an edge dislocation and a nanosized circular

* Corresponding author.
E-mail addresses: xuwang@ecust.edu.cn (X. Wang), cuiyingwang@126.com (C. Wang), p.schiavone@ualberta.ca (P. Schiavone).

http://dx.doi.org/10.1016/j.euromechsol.2016.09.008
0997-7538/

inhomogeneity. The inhomogeneity and the matrix are first endowed with separate and distinct surface elasticities and are then bonded through an imperfect interface permitting rate-dependent slip and diffusion. An analytical solution in series form to this interaction problem is derived by means of complex variable methods. In contrast to the previous analysis in Wang and Pan (2010, 2011), we propose a simple yet effective method based on analytical continuation and a convenient decomposition of the solution which allows us to circumvent the involvement of the second-order tangential derivative (taken with respect to interfacial normal stress) normally appearing in the description of interface diffusion. This method has been adopted in a recent analysis of a nanosized circular inhomogeneity with interface slip and diffusion in the case when the surrounding matrix is subjected to uniform remote stresses (Wang et al., 2016). The time-dependent image force acting on the edge dislocation is then obtained using the acquired solution and the Peach-Koehler formula (Dundurs, 1969). We also present the asymptotic expression for the image force when the dislocation is located far from the inhomogeneity. Our analysis indicates that the stress and displacement fields in the composite as well as the normalized image force acting on the edge dislocation are dependent on four size-dependent dimensionless parameters γ_1, γ_2, δ_1, δ_2 arising from the surface elasticities and on two size-dependent parameters ρ, χ (having the dimension of time) arising from interface slip and diffusion and they evolve with an infinite number of relaxation times. These relaxation times rely, in turn, on the two size-dependent dimensionless parameters γ_1, γ_2 (arising from the surface elasticities) and on the two size-dependent parameters ρ, χ associated with interface slip and diffusion. Due to the existence of residual surface tensions, the normalized image force acting on a climbing dislocation, the Burgers vector of which is directed tangentially to the interface, is no longer an odd function of the dislocation position parameter and is actually dependent on a further size-dependent parameter which is given by the ratio of the radius of the inhomogeneity to the Burgers vector. We also present long range interaction results both in time and in space.

2. The coupled bulk-surface elasticity, interface slip and diffusion

In this section, the basic formulations describing the bulk elasticity, the surface elasticity and interface slip and diffusion are briefly summarized.

2.1. The bulk elasticity

In what follows, unless otherwise stated, Latin indices *i,j,k* take the values 1,2,3 and we sum over repeated indices. In the absence of body forces, the equilibrium equations and the stress-strain law describing the deformation of a linearly elastic, homogeneous and isotropic bulk solid can be expressed in a fixed rectangular coordinate system $\{x_i\}$ as follows

$$\sigma_{ij,j}=0,\quad \sigma_{ij}=2\mu\varepsilon_{ij}+\lambda\varepsilon_{kk}\delta_{ij},\quad \varepsilon_{ij}=\frac{1}{2}\left(u_{i,j}+u_{j,i}\right), \tag{1}$$

where λ and μ are Lame constants, σ_{ij} and ε_{ij} are, respectively, the Cartesian components of the stress and strain tensors in the bulk material, u_i is the i-th component of the displacement vector and δ_{ij} is the Kronecker delta.

For plane-strain problems, the stresses, displacements and stress functions φ_1, φ_2 can be expressed in terms of two analytic functions $\phi(z)$ and $\psi(z)$ of the complex variable $z=x_1+\mathrm{i}x_2$ as (Muskhelishvili, 1953; Ting, 1996)

$$\begin{aligned}
&\sigma_{11}+\sigma_{22}=2\left[\phi'(z)+\overline{\phi'(z)}\right],\\
&\sigma_{22}-\sigma_{11}+2\mathrm{i}\sigma_{12}=2\left[\bar{z}\phi''(z)+\psi'(z)\right],\\
&2\mu(u_1+\mathrm{i}u_2)=\kappa\phi(z)-z\overline{\phi'(z)}-\overline{\psi(z)},\\
&\varphi_1+\mathrm{i}\varphi_2=\mathrm{i}\left[\phi(z)+z\overline{\phi'(z)}+\overline{\psi(z)}\right],
\end{aligned} \tag{2}$$

where $\kappa=3-4\nu$ and ν ($0\le\nu\le 1/2$) is Poisson's ratio. In addition, the stresses are related to the stress functions through (Ting, 1996)

$$\begin{aligned}
&\sigma_{11}=-\varphi_{1,2},\quad \sigma_{12}=\varphi_{1,1},\\
&\sigma_{21}=-\varphi_{2,2},\quad \sigma_{22}=\varphi_{2,1}.
\end{aligned} \tag{3}$$

Let T_1 and T_2 be traction components along the x_1-and x_2-directions on a boundary L. If s is the arc-length measured along L such that the material remains on the left-hand side in the direction of increasing s, it can be shown that (Ting, 1996)

$$T_1+\mathrm{i}T_2=-\frac{d(\varphi_1+\mathrm{i}\varphi_2)}{ds}. \tag{4}$$

2.2. The surface elasticity

The equilibrium conditions on the surface incorporating interface/surface elasticity can be expressed as (Gurtin and Murdoch, 1975, 1978; Gurtin et al., 1998; Ru, 2010)

$$\begin{aligned}
&\left[\sigma_{\alpha j}n_j\underline{e}_\alpha\right]+\sigma^s_{\alpha\beta,\beta}\underline{e}_\alpha=0, \quad \text{(tangential direction)}\\
&\left[\sigma_{ij}n_in_j\right]=\sigma^s_{\alpha\beta}\kappa_{\alpha\beta}, \quad \text{(normal direction)}
\end{aligned} \tag{5}$$

where n_i are the components of the unit normal vector to the surface, [*] denotes the jump of the respective quantity across the surface, $\sigma^s_{\alpha\beta}$ are the Cartesian components of the surface stress tensor and $\kappa_{\alpha\beta}$ is the curvature tensor of the surface. In addition, the constitutive equations on the isotropic surface are given by

$$\sigma^s_{\alpha\beta}=\sigma_0\delta_{\alpha\beta}+2(\mu_s-\sigma_0)\varepsilon^s_{\alpha\beta}+(\lambda_s+\sigma_0)\varepsilon^s_{\gamma\gamma}\delta_{\alpha\beta}, \tag{6}$$

where $\varepsilon^s_{\alpha\beta}$ are the components of the surface strain tensor, σ_0 is the surface tension and λ_s and μ_s are the two surface Lame constants.

We mention that in Eqs. (5) and (6), the Greek indices α, β and γ take on values of the surface components. For example, in the case of circular cylindrical fibers, α, β, γ each take on the values θ, z.

2.3. Interface slip and diffusion

Let u_r and u_θ be the components of the displacement vector, normal and tangential, respectively, to the inhomogeneity-matrix interface L and σ_{rr},$\sigma_{r\theta}$ the normal and shear components, respectively, of the traction along the interface L. The interface slip and interface diffusion boundary conditions can then be explicitly expressed as (Koeller and Raj, 1978; Sofronis and McMeeking, 1994; Kim and McMeeking, 1995; Onaka et al., 1998; Wei et al., 2008)

$$[\sigma_{rr}+\mathrm{i}\sigma_{r\theta}]=0,\quad \sigma_{r\theta}=\vartheta[\dot{u}_\theta],\quad D\frac{d^2\sigma_{rr}}{ds^2}=-[\dot{u}_r],\quad \text{on } L, \tag{7}$$

where the overdot denotes differentiation with respect to time t, ϑ is the non-negative interface drag constant, D is the non-negative interface diffusion constant, and $[*]=[*]_M-[*]_I$ describes the jump across L. The definition of s in Eq. (7) is the same as that in Eq. (4). The interface slip is absent when $\vartheta\to\infty$; the interface diffusion is absent when $D=0$; the interface slip occurs much faster than the interface diffusion when $\vartheta=0$; the interface diffusion occurs much faster than the interface slip when $D\to\infty$. The appearance of the

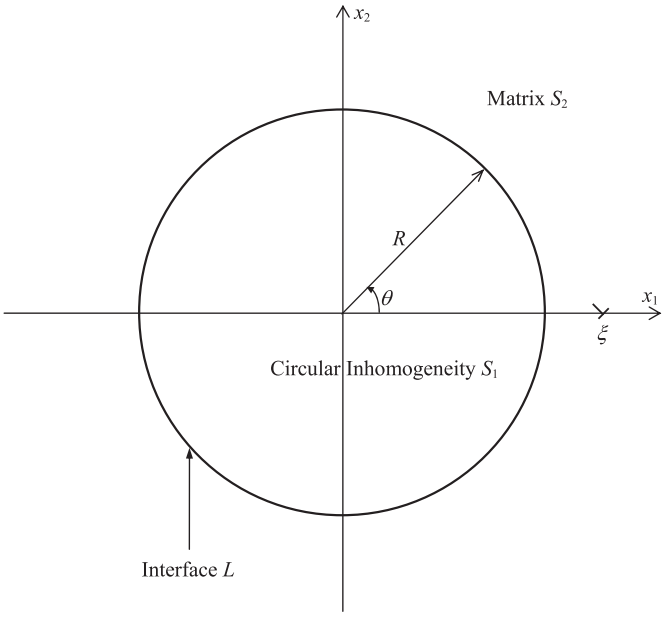

Fig. 1. An edge dislocation near a nanosized circular inhomogeneity with interface slip and diffusion.

second-order tangential derivative with respect to the interfacial normal stress in Eq. (7) will result in an extremely complicated and tedious expression (Wang and Pan, 2010, 2011) when the interface conditions are written in terms of the corresponding analytic functions. Alternatively, in this paper, we propose a simple yet effective method to circumvent this difficulty.

3. An edge dislocation near a nanosized circular inhomogeneity with interface slip and diffusion

Consider a nanosized circular elastic inhomogeneity embedded in an infinite elastic matrix as shown in Fig. 1. We represent the matrix by the domain S_2 and assume that the inhomogeneity occupies a circular region S_1 of radius R with its centre at the origin of the coordinate system. The inhomogeneity-matrix interface is denoted by L. In what follows, the subscripts 1 and 2 (or the superscripts (1) and (2)) are used to identify the respective quantities in S_1 and S_2. Separate Gurtin-Murdoch surface elasticities are simultaneously incorporated onto the surface of the inhomogeneity and onto that of the matrix. Moreover, the two phases are bonded through an imperfect interface permitting interface slip and diffusion. An edge dislocation with Burgers vector $(b_1,\ b_2)$ is located at $(\xi,\ 0)$ on the x_1-axis in the matrix. No other external loading is applied to the composite.

By assuming that the interface L is coherent with respect to either the inhomogeneity or the matrix, it then follows from Eqs. (5) and (6) that the boundary conditions on the surface of the circular inhomogeneity and on that of the matrix can be written specifically as

$$\begin{aligned}\left(\sigma_{rr}^{(1)}+\mathrm{i}\sigma_{r\theta}^{(1)}\right)-\left(\sigma_{rr}^{-}+\mathrm{i}\sigma_{r\theta}^{-}\right)&=-\frac{\sigma_0^{(1)}}{R}\\&+\frac{J_0^{(1)}}{R^2}\left[\mathrm{i}\frac{d^2u_\theta^{(1)}}{d\theta^2}+\mathrm{i}\frac{d\left(u_r^{(1)}+\mathrm{i}u_\theta^{(1)}\right)}{d\theta}-u_r^{(1)}\right],\\&\text{on the surface of the inhomogeneity,}\end{aligned}\tag{8}$$

$$\begin{aligned}\left(\sigma_{rr}^{+}+\mathrm{i}\sigma_{r\theta}^{+}\right)-\left(\sigma_{rr}^{(2)}+\mathrm{i}\sigma_{r\theta}^{(2)}\right)&=-\frac{\sigma_0^{(2)}}{R}\\&+\frac{J_0^{(2)}}{R^2}\left[\mathrm{i}\frac{d^2u_\theta^{(2)}}{d\theta^2}+\mathrm{i}\frac{d\left(u_r^{(2)}+\mathrm{i}u_\theta^{(2)}\right)}{d\theta}-u_r^{(2)}\right],\\&\text{on the surface of the matrix,}\end{aligned}\tag{9}$$

where $J_0^{(j)}=2\mu_s^{(j)}+\lambda_s^{(j)}-\sigma_0^{(j)}\geq 0,\ j=1,\ 2$, and

$$\begin{aligned}&\sigma_{r\theta}^{-}=\sigma_{r\theta}^{+}=\vartheta\left(\dot{u}_\theta^{(2)}-\dot{u}_\theta^{(1)}\right),\quad \frac{D}{R^2}\frac{d^2\sigma_{rr}^{-}}{d\theta^2}=\frac{D}{R^2}\frac{d^2\sigma_{rr}^{+}}{d\theta^2}\\&=\dot{u}_r^{(1)}-\dot{u}_r^{(2)},\ \text{on } L,\end{aligned}\tag{10}$$

according to Eq. (7).

In order to solve the ensuing boundary value problem, we introduce the following analytical continuations:

$$\begin{aligned}\phi_1(z)&=-z\overline{\phi}'_1\left(R^2/z\right)-\overline{\psi}_1\left(R^2/z\right),\quad |z|>R,\\ \phi_2(z)&=-z\overline{\phi}'_2\left(R^2/z\right)-\overline{\psi}_2\left(R^2/z\right),\quad |z|<R.\end{aligned}\tag{11}$$

The two analytic functions $\phi_1(z),\ \phi_2(z)$ and their analytical continuations can be written in the following form:

$$\phi_1(z)=\begin{cases}\sum\limits_{n=0}^{+\infty}X_nR^{-n}z^n, & |z|<R,\\ -\overline{X}_1R^{-1}z+\sum\limits_{n=0}^{+\infty}Y_nR^nz^{-n}, & |z|>R,\end{cases}$$

$$\phi_2(z)=\begin{cases}-A\log\dfrac{z-R^2/\xi}{z}+\dfrac{R^2\left(R^2-\xi^2\right)}{\xi^3}\dfrac{\overline{A}}{z-R^2/\xi}\\ \quad+\sum\limits_{n=0}^{+\infty}B_nR^{-n}z^n, & |z|<R,\\ A\log(z-\xi)+\sum\limits_{n=0}^{+\infty}A_nR^nz^{-n}, & |z|>R,\end{cases}\tag{12}$$

where $X_n,\ Y_n,\ A_n, B_n,\ n=0,\ 1,\ 2,\cdots,\ +\infty$ are unknown complex coefficients to be determined and

$$A=\frac{\mu_2(b_2-\mathrm{i}b_1)}{\pi(\kappa_2+1)}.\tag{13}$$

The logarithmic functions and the first-order poles at $z=\xi$ and $z=R^2/\xi$ in Eq. (12) can be expanded into convergent Laurent series within the thin annulus $R-\varepsilon<|z|<R+\varepsilon$ with ε an extremely small positive number. Consequently, Eq. (12) can be decomposed into

$$\phi_1(z)=\sum_{n=1}^{+\infty}\phi_1^{(n)}(z),\quad \phi_2(z)=\sum_{n=1}^{+\infty}\phi_2^{(n)}(z),\tag{14}$$

where

$$\begin{aligned}\phi_1^{(1)}(z)&=\begin{cases}X_1R^{-1}z, & R-\varepsilon<|z|<R,\\ -\overline{X}_1R^{-1}z, & R<|z|<R+\varepsilon,\end{cases}\\ \phi_2^{(1)}(z)&=\begin{cases}B_1R^{-1}z, & R-\varepsilon<|z|<R,\\ E_1R^{-1}z, & R<|z|<R+\varepsilon,\end{cases}\end{aligned}\tag{15}$$

$$\phi_1^{(2)}(z)=\begin{cases} X_0+X_2R^{-2}z^2, & R-\varepsilon<|z|<R,\\ Y_0, & R<|z|<R+\varepsilon,\end{cases}$$
$$\phi_2^{(2)}(z)=\begin{cases} B_0+B_2R^{-2}z^2, & R-\varepsilon<|z|<R,\\ A_0+E_0+E_2R^{-2}z^2, & R<|z|<R+\varepsilon,\end{cases} \tag{16}$$

respectively.

Substituting Eq. (15) into Eq. (20), equating coefficients of like powers of z and solving the resulting two coupled linear algebraic equations, we finally arrive at the expressions of the two coefficients X_1 and B_1 as follows

$$X_1=\frac{\Gamma E'_1(\kappa_2+1)-2R\mu_1(\Gamma\delta_1+\delta_2)}{2\Gamma+(\kappa_1-1)(1+\Gamma\gamma_1+\gamma_2)}+\mathrm{i}\frac{\Gamma(\kappa_2+1)}{\kappa_1+1}E''_1,$$
$$B_1=\frac{E'_1[\kappa_1-1-2\Gamma\kappa_2-\kappa_2(\kappa_1-1)(\Gamma\gamma_1+\gamma_2)]-2R\mu_2(\kappa_1-1)(\Gamma\delta_1+\delta_2)}{2\Gamma+(\kappa_1-1)(1+\Gamma\gamma_1+\gamma_2)}+\mathrm{i}E''_1, \tag{21}$$

$$\phi_1^{(n)}(z)=\begin{cases} X_nR^{-n}z^n, & R-\varepsilon<|z|<R,\\ Y_{n-2}R^{n-2}z^{2-n}, & R<|z|<R+\varepsilon,\end{cases}$$
$$n=3,4,\cdots,+\infty,$$
$$\phi_2^{(n)}(z)=\begin{cases} F_{n-2}R^{n-2}z^{2-n}+B_nR^{-n}z^n, & R-\varepsilon<|z|<R,\\ E_nR^{-n}z^n+A_{n-2}R^{n-2}z^{2-n}, & R<|z|<R+\varepsilon,\end{cases} \tag{17}$$

where the known loading parameters $E_0,\ E_n,\ F_n,\ n=1,\ 2,\cdots,\ +\infty$ are given by

$$E_0=A\log(-\xi),\quad E_n=-\frac{A}{n}\left(\frac{R}{\xi}\right)^n,$$
$$F_n=\left(\frac{A}{n}-\overline{A}\right)\left(\frac{R}{\xi}\right)^n+\overline{A}\left(\frac{R}{\xi}\right)^{n+2},\quad n=1,\ 2,\cdots,\ +\infty. \tag{18}$$

When we choose $\phi_1(z)=\phi_1^{(1)}(z)$ and $\phi_2(z)=\phi_2^{(1)}(z)$, both the interface slip and diffusion are absent. If we assume that $u_r^{(1)}=u_r^{(2)}$ and $u_\theta^{(1)}=u_\theta^{(2)}$ on L at the initial instant $t=0$, the interface conditions in Eqs. (8) and (9) now become

$$u_r^{(1)}+\mathrm{i}u_\theta^{(1)}=u_r^{(2)}+\mathrm{i}u_\theta^{(2)},$$
$$\left(\sigma_{rr}^{(1)}+\mathrm{i}\sigma_{r\theta}^{(1)}\right)-\left(\sigma_{rr}^{(2)}+\mathrm{i}\sigma_{r\theta}^{(2)}\right)=-\frac{\sigma_0^{(1)}+\sigma_0^{(2)}}{R}$$
$$+\frac{J_0^{(1)}+J_0^{(2)}}{R^2}\left[\mathrm{i}\frac{d^2u_\theta^{(1)}}{d\theta^2}+\mathrm{i}\frac{d\left(u_r^{(1)}+\mathrm{i}u_\theta^{(1)}\right)}{d\theta}-u_r^{(1)}\right],\ \text{on } L, \tag{19}$$

which can be simply expressed in terms of $\phi_1(z),\ \phi_2(z)$ and their analytic continuations as follows:

$$\frac{1}{2\mu_1}\left[\kappa_1\phi_1^+(z)+\phi_1^-(z)\right]=\frac{1}{2\mu_2}\left[\kappa_2\phi_2^-(z)+\phi_2^+(z)\right],$$
$$\phi'^+_1(z)-\phi'^-_1(z)+\phi'^+_2(z)-\phi'^-_2(z)=-\frac{\sigma_0^{(1)}+\sigma_0^{(2)}}{R}$$
$$-\frac{J_0^{(1)}+J_0^{(2)}}{2R\mu_1}\mathrm{Re}\left\{\kappa_1z^{-1}\phi_1^+(z)+z^{-1}\phi_1^-(z)\right\},$$
$$|z|=R, \tag{20}$$

where the superscripts "+" and "−" indicate the limiting values as we approach the interface L from the inside and outside,

where E'_1 and E''_1 are, respectively, the real and imaginary parts of E_1, and

$$\gamma_1=\frac{J_0^{(1)}}{2R\mu_1},\quad \delta_1=\frac{\sigma_0^{(1)}}{2R\mu_1},\quad \gamma_2=\frac{J_0^{(2)}}{2R\mu_2},\quad \delta_2=\frac{\sigma_0^{(2)}}{2R\mu_2},\quad \Gamma=\frac{\mu_1}{\mu_2}. \tag{22}$$

The four size-dependent dimensionless parameters $\gamma_1,\ \delta_1,\ \gamma_2$ and δ_2 defined in Eq. (22) arise from the incorporation of surface elasticities. They are inversely proportional to R. Clearly both X_1 and B_1 obtained in Eq. (21) are time-independent.

When we choose $\phi_1(z)=\phi_1^{(n)}(z)$ and $\phi_2(z)=\phi_2^{(n)}(z)$ with $n\geq 2$, the interface slip and diffusion conditions in Eq. (10) can be equivalently expressed in the following form for any fixed value of $n(\geq 2)$

$$\sigma_{rr}^- +\mathrm{i}\sigma_{r\theta}^- =\sigma_{rr}^+ +\mathrm{i}\sigma_{r\theta}^+ =\left[\frac{R^2}{2D(n-1)^2}+\frac{\vartheta}{2}\right]\left[\left(\dot{u}_r^{(2)}+\mathrm{i}\dot{u}_\theta^{(2)}\right)\right.$$
$$\left.-\left(\dot{u}_r^{(1)}+\mathrm{i}\dot{u}_\theta^{(1)}\right)\right]+\left[\frac{R^2}{2D(n-1)^2}-\frac{\vartheta}{2}\right]\left[\left(\dot{u}_r^{(2)}-\mathrm{i}\dot{u}_\theta^{(2)}\right)\right.$$
$$\left.-\left(\dot{u}_r^{(1)}-\mathrm{i}\dot{u}_\theta^{(1)}\right)\right],\ \text{on } L. \tag{23}$$

Consequently, the boundary conditions in Eqs. (8), (9) and (23) can be written in terms of $\phi_1(z),\ \phi_2(z)$ and their analytic continuations as follows:

$$\phi'^+_1(z)-\phi'^-_1(z)-\left[\frac{R^2}{4D(n-1)^2}+\frac{\vartheta}{4}\right]\left[\frac{R}{\mu_2}\left(\kappa_2z^{-1}\dot{\phi}_2^-(z)+z^{-1}\dot{\phi}_2^+(z)\right)\right.$$
$$\left.-\frac{R}{\mu_1}\left(\kappa_1z^{-1}\dot{\phi}_1^+(z)+z^{-1}\dot{\phi}_1^-(z)\right)\right]$$
$$-\left[\frac{R^2}{4D(n-1)^2}-\frac{\vartheta}{4}\right]\left[\frac{R^{-1}}{\mu_2}\left(\kappa_2z\dot{\bar{\phi}}_2^+\left(R^2/z\right)+z\dot{\bar{\phi}}_2^-\left(R^2/z\right)\right)\right.$$
$$\left.-\frac{R^{-1}}{\mu_1}\left(\kappa_1z\dot{\bar{\phi}}_1^-\left(R^2/z\right)+z\dot{\bar{\phi}}_1^+\left(R^2/z\right)\right)\right]$$
$$=\frac{J_0^{(1)}}{2R\mu_1}\begin{pmatrix}-\mathrm{iIm}\left\{\kappa_1z^{-1}\phi_1^+(z)-\kappa_1\phi'^+_1(z)+\kappa_1z\phi''^+_1(z)\right.\\ \left.+z^{-1}\phi_1^-(z)-\phi'^-_1+z\phi''^-_1(z)\right\}\\ +\kappa_1z^{-1}\phi_1^+(z)-\kappa_1\phi'^+_1(z)+z^{-1}\phi_1^-(z)-\phi'^-_1(z)\\ -\mathrm{Re}\left\{\kappa_1z^{-1}\phi_1^+(z)+z^{-1}\phi_1^-(z)\right\}\end{pmatrix},$$
$$|z|=R, \tag{24}$$

$$\phi_2'^{+}(z)-\phi_2'^{-}(z)+\left[\frac{R^2}{4D(n-1)^2}+\frac{\vartheta}{4}\right]\left[\frac{R}{\mu_2}\left(\kappa_2 z^{-1}\dot{\phi}_2^{-}(z)+z^{-1}\dot{\phi}_2^{+}(z)\right)-\frac{R}{\mu_1}\left(\kappa_1 z^{-1}\dot{\phi}_1^{+}(z)+z^{-1}\dot{\phi}_1^{-}(z)\right)\right]$$
$$+\left[\frac{R^2}{4D(n-1)^2}-\frac{\vartheta}{4}\right]\left[\frac{R^{-1}}{\mu_2}\left(\kappa_2 z\dot{\bar{\phi}}_2^{+}\left(R^2/z\right)+z\dot{\bar{\phi}}_2^{-}\left(R^2/z\right)\right)-\frac{R^{-1}}{\mu_1}\left(\kappa_1 z\dot{\bar{\phi}}_1^{-}\left(R^2/z\right)+z\dot{\bar{\phi}}_1^{+}\left(R^2/z\right)\right)\right]$$
$$=\frac{J_0^{(2)}}{2R\mu_2}\begin{pmatrix}-\mathrm{iIm}\left\{\kappa_2 z^{-1}\phi_2^{-}(z)-\kappa_2\phi_2'^{-}(z)+\kappa_2 z\phi_2''^{-}(z)+z^{-1}\phi_2^{+}(z)-\phi_2'^{+}(z)+z\phi_2''^{+}(z)\right\}\\ +\kappa_2 z^{-1}\phi_2^{-}(z)-\kappa_2\phi_2'^{-}(z)+z^{-1}\phi_2^{+}(z)-\phi_2'^{+}(z)-\mathrm{Re}\left\{\kappa_2 z^{-1}\phi_2^{-}(z)+z^{-1}\phi_2^{+}(z)\right\}\end{pmatrix},$$

$$|z|=R. \tag{25}$$

Substituting Eq. (16) for $n=2$ into Eqs. (24) and (25), equating coefficients of z and z^{-1}, we arrive at the following set of state-space equations for the variables X_2, B_2 and $\kappa_1X_0+Y_0-\Gamma(\kappa_2A_0+B_0)$

$$\begin{aligned}&(1+\kappa_1\gamma_1)X_2+\frac{\rho\chi}{\rho-\chi}\left[\Gamma\left(\kappa_2\dot{\bar{A}}_0+\dot{\bar{B}}_0\right)-\left(\kappa_1\dot{\bar{X}}_0+\dot{\bar{Y}}_0\right)\right]=0,\\ &(1+\gamma_2)B_2-\frac{\rho\chi}{\rho-\chi}\left[\Gamma\left(\kappa_2\dot{\bar{A}}_0+\dot{\bar{B}}_0\right)-\left(\kappa_1\dot{\bar{X}}_0+\dot{\bar{Y}}_0\right)\right]=(1-\gamma_2\kappa_2)E_2,\\ &\Gamma\dot{B}_2-\kappa_1\dot{X}_2=-\frac{\rho+\chi}{\rho-\chi}\left[\Gamma\left(\kappa_2\dot{\bar{A}}_0+\dot{\bar{B}}_0\right)-\left(\kappa_1\dot{\bar{X}}_0+\dot{\bar{Y}}_0\right)\right],\end{aligned} \tag{26}$$

where

$$\rho=\frac{R^3}{2\mu_1 D},\quad \chi=\frac{R\vartheta}{2\mu_1}. \tag{27}$$

The above introduced two size-dependent parameters ρ and χ have the dimension of time. In addition, ρ is proportional to R^3 whilst χ is proportional to R. By assuming that initially ($t=0$), $u_r^{(1)}=u_r^{(2)}$ and $u_\theta^{(1)}=u_\theta^{(2)}$ on L, the three time-dependent coefficients X_2, B_2 and $\kappa_1X_0+Y_0-\Gamma(\kappa_2A_0+B_0)$ can be obtained as

$$\begin{aligned}&B_2=-\frac{E_2\Gamma(\kappa_2+1)(1+\kappa_1\gamma_1)}{(1+\gamma_2)[\Gamma+\kappa_1(1+\Gamma\gamma_1+\gamma_2)]}\mathrm{e}^{-t/t_0}+\frac{E_2(1-\gamma_2\kappa_2)}{1+\gamma_2},\\ &X_2=\frac{E_2\Gamma(\kappa_2+1)}{\Gamma+\kappa_1(1+\Gamma\gamma_1+\gamma_2)}\mathrm{e}^{-t/t_0},\\ &\kappa_1X_0+Y_0-\Gamma(\kappa_2A_0+B_0)=\frac{\bar{E}_2\Gamma(\kappa_2+1)(\rho-\chi)}{(1+\gamma_2)(\rho+\chi)}\left(1-\mathrm{e}^{-t/t_0}\right)+\Gamma\kappa_2E_0,\end{aligned} \tag{28}$$

where

$$t_0=\frac{\Gamma+\kappa_1(1+\Gamma\gamma_1+\gamma_2)}{(1+\kappa_1\gamma_1)(1+\gamma_2)}\frac{\rho\chi}{\rho+\chi}. \tag{29}$$

The relaxation time t_0 is dependent on four size-dependent parameters: the two dimensionless parameters γ_1, γ_2 arising from surface elasticities and the remaining two parameters ρ, χ due to interface slip and diffusion. Consequently t_0 is size-dependent. It is quite straightforward to show that the existence of surface elasticities will lower the value of the relaxation time, i.e., $t_0<\rho\chi(\Gamma+\kappa_1)/(\rho+\chi)$.

Substituting Eq. (17) for $n\geq 3$ into Eqs. (24) and (25), equating coefficients of z^{n-1} and z^{1-n}, we finally obtain the following sets of state-space equations:

$$\begin{aligned}&\mathbf{P}_n\begin{bmatrix}\kappa_1\dot{X}_n\\ \dot{\bar{Y}}_{n-2}\\ \Gamma\dot{B}_n\\ \Gamma\kappa_2\dot{\bar{A}}_{n-2}\end{bmatrix}+\mathbf{Q}_n\begin{bmatrix}\kappa_1X_n\\ \bar{Y}_{n-2}\\ \Gamma B_n\\ \Gamma\kappa_2\bar{A}_{n-2}\end{bmatrix}\\ &\quad=\begin{bmatrix}0\\ 0\\ n(2-n\kappa_2\gamma_2)E_n+\gamma_2n(n-2)\bar{F}_{n-2}\\ \kappa_2\gamma_2n(n-2)E_n+\left[2(n-2)-\gamma_2(n-2)^2\right]\bar{F}_{n-2}\end{bmatrix},\end{aligned}$$

$$n=3,\ 4,\cdots,\ +\infty, \tag{30}$$

where

$$\mathbf{P}_n=\mathbf{P}_n^T=\begin{bmatrix}\rho_n+\chi & \rho_n-\chi & -(\rho_n+\chi) & \chi-\rho_n\\ \rho_n-\chi & \rho_n+\chi & \chi-\rho_n & -(\rho_n+\chi)\\ -(\rho_n+\chi) & \chi-\rho_n & \rho_n+\chi & \rho_n-\chi\\ \chi-\rho_n & -(\rho_n+\chi) & \rho_n-\chi & \rho_n+\chi\end{bmatrix},$$

$$\mathbf{Q}_n=\mathbf{Q}_n^T=\begin{bmatrix}\frac{2n}{\kappa_1}+\gamma_1n^2 & -\gamma_1n(n-2) & 0 & 0\\ -\gamma_1n(n-2) & 2(n-2)+\gamma_1(n-2)^2 & 0 & 0\\ 0 & 0 & \frac{2n+\gamma_2n^2}{\Gamma} & -\frac{\gamma_2n(n-2)}{\Gamma}\\ 0 & 0 & -\frac{\gamma_2n(n-2)}{\Gamma} & \frac{2(n-2)}{\Gamma\kappa_2}+\frac{\gamma_2(n-2)^2}{\Gamma}\end{bmatrix}, \tag{31}$$

with

$$\rho_n = \frac{R^3}{2\mu_1 D(n-1)^2} = \frac{\rho}{(n-1)^2}. \tag{32}$$

where

$$c_2 = n(n-2)[2+\gamma_1(n\kappa_1+n-2)][2+\gamma_2[n+\kappa_2(n-2)]],$$

$$c_1 = \frac{\rho}{(n-1)^2}\begin{pmatrix} 2(n-2)(\Gamma+\kappa_1)+2n(\Gamma\kappa_2+1) \\ +\gamma_1\left\{\Gamma(n-2)^2+\kappa_1\left[4(n-1)^2+\Gamma n(n-2)\right]+\Gamma\kappa_2 n(n-2)+\Gamma\kappa_1\kappa_2 n^2\right\} \\ +\gamma_2\left\{n^2+\kappa_1 n(n-2)+\kappa_2\left[n(n-2)+4\Gamma(n-1)^2\right]+\kappa_1\kappa_2(n-2)^2\right\} \\ +2\gamma_1\gamma_2(n-1)^2[n\kappa_1+\Gamma\kappa_2(n-2)+\kappa_1\kappa_2(\Gamma n+n-2)] \end{pmatrix}$$

$$+\chi\begin{pmatrix} 2(n-2)(\Gamma+\kappa_1)+2n(\Gamma\kappa_2+1) \\ +\gamma_1\left[\Gamma(n-2)^2+\kappa_1[4+\Gamma n(n-2)]+\Gamma\kappa_2 n(n-2)+\Gamma\kappa_1\kappa_2 n^2\right] \\ +\gamma_2\left[n^2+\kappa_1 n(n-2)+\kappa_2[n(n-2)+4\Gamma]+\kappa_1\kappa_2(n-2)^2\right] \\ +2\gamma_1\gamma_2[n\kappa_1+\Gamma\kappa_2(n-2)+\kappa_1\kappa_2(n-2+n\Gamma)] \end{pmatrix}, \tag{35}$$

$$c_0 = \frac{2\rho\chi}{(n-1)^2}\{2(\Gamma+\kappa_1)(\Gamma\kappa_2+1)+(\Gamma\gamma_1+\gamma_2)[n\kappa_1(\Gamma\kappa_2+1)+\kappa_2(n-2)(\Gamma+\kappa_1)]\}.$$

It can be shown that the 4×4 real symmetric matrix $\mathbf{P}_n$ is positive semi-definite, and that the 4×4 real symmetric matrix $\mathbf{Q}_n$ is positive definite. In order to solve the state-space equations in Eq. (30), we first consider the following generalized eigenvalue problem:

$$(\mathbf{P}_n - \lambda\mathbf{Q}_n)\mathbf{v} = 0, \tag{33}$$

where λ is the eigenvalue and $\mathbf{v}$ the associated eigenvector. After some lengthy but straightforward algebraic manipulations, the four eigenvalues of Eq. (33) can be explicitly determined as

$$\lambda_1 = \frac{c_1+\sqrt{c_1^2-4c_0c_2}}{2c_2} > 0, \quad \lambda_2 = \frac{c_1-\sqrt{c_1^2-4c_0c_2}}{2c_2} > 0,$$
$$\lambda_3 = \lambda_4 = 0, \tag{34}$$

The correctness of Eqs. (34) and (35) has been verified numerically by using Matlab. We denote $t_n^+ = \lambda_1$, $t_n^- = \lambda_2$, and let $\mathbf{v}_n^+$, $\mathbf{v}_n^-$ be the eigenvectors associated with the two positive eigenvalues. The two eigenvectors $\mathbf{v}_n^+$, $\mathbf{v}_n^-$ can be explicitly written as

$$\mathbf{v}_n^+ = \begin{bmatrix} \mathbf{w}_n^+ \\ 1 \end{bmatrix}, \quad \mathbf{v}_n^- = \begin{bmatrix} \mathbf{w}_n^- \\ 1 \end{bmatrix}, \tag{36}$$

where

$$\mathbf{w}_n^\pm = \begin{bmatrix} \rho_n+\chi-t_n^\pm\left(\frac{2n}{\kappa_1}+\gamma_1 n^2\right) & \rho_n-\chi+t_n^\pm\gamma_1 n(n-2) & -(\rho_n+\chi) \\ \rho_n-\chi+t_n^\pm\gamma_1 n(n-2) & \rho_n+\chi-t_n^\pm\left[2(n-2)+\gamma_1(n-2)^2\right] & \chi-\rho_n \\ -(\rho_n+\chi) & \chi-\rho_n & \rho_n+\chi-\frac{t_n^\pm(2n+\gamma_2 n^2)}{\Gamma} \end{bmatrix}^{-1}$$
$$\times\begin{bmatrix} \rho_n-\chi \\ \rho_n+\chi \\ \chi-\rho_n-\frac{t_n^\pm\gamma_2 n(n-2)}{\Gamma} \end{bmatrix}. \tag{37}$$

After inverting the 3 × 3 symmetric matrix in Eq. (37) and carrying out some lengthy algebraic manipulations, we can obtain the three components of $\mathbf{w}_n^{\pm}$ (their explicit expressions are listed in the Appendix). The general solution to Eq. (30) can then be written as

$$\psi_1(z) = -\sum_{n=0}^{+\infty}\left[\overline{Y}_n + (n+2)X_{n+2}\right]R^{-n}z^n, \qquad |z|<R;$$

$$\psi_2(z) = \overline{A}\log(z-\xi) - \frac{\xi A}{z-\xi} - \left[\overline{A}\log(-\xi) + \frac{A\left(\xi^2-R^2\right)}{\xi^2} + \overline{B}_0\right] + \left(\frac{R}{\xi}A - \overline{B}_1\right)Rz^{-1} + \sum_{n=2}^{+\infty}\left[(n-2)A_{n-2} - \overline{B}_n\right]R^n z^{-n}, \qquad |z|>R. \tag{43}$$

$$\begin{bmatrix} \kappa_1 X_n \\ \overline{Y}_{n-2} \\ \Gamma\overline{B}_n \\ \Gamma\kappa_2\overline{A}_{n-2} \end{bmatrix} = d_1\mathbf{v}_n^{+}\mathrm{e}^{-t/t_n^{+}} + d_2\mathbf{v}_n^{-}\mathrm{e}^{-t/t_n^{-}} + \frac{\Gamma}{2+\gamma_2[n+\kappa_2(n-2)]}\begin{bmatrix} 0 \\ 0 \\ 2(1-\gamma_2\kappa_2)E_n + \gamma_2(n-2)(1+\kappa_2)\overline{F}_{n-2} \\ n\gamma_2\kappa_2(1+\kappa_2)E_n + 2\kappa_2(1+\gamma_2)\overline{F}_{n-2} \end{bmatrix}, \tag{38}$$

where d_1 and d_2 are two unknown time-independent constants to be determined through the satisfaction of the initial conditions. It is seen from Eqs. (34) and (35) that the two relaxation times t_n^{+} and t_n^{-} are dependent on the four size-dependent parameters γ_1, γ_2, ρ and χ.

If we assume that $u_r^{(1)} = u_r^{(2)}$ and $u_\theta^{(1)} = u_\theta^{(2)}$ on L at time $t = 0$, we have

$$\begin{aligned} \kappa_1 X_n &= \frac{\Gamma\kappa_1(\kappa_2+1)\{E_n[2(\Gamma\kappa_2+1)+\kappa_2(n-2)(\Gamma\gamma_1+\gamma_2)] + \overline{F}_{n-2}(n-2)(\Gamma\gamma_1+\gamma_2)\}}{2(\Gamma+\kappa_1)(\Gamma\kappa_2+1)+(\Gamma\gamma_1+\gamma_2)[n\kappa_1+\Gamma\kappa_2(n-2)+\kappa_1\kappa_2(n-2+n\Gamma)]}, \\ \overline{Y}_{n-2} &= \frac{\Gamma(\kappa_2+1)\{E_n n\kappa_1\kappa_2(\Gamma\gamma_1+\gamma_2) + \overline{F}_{n-2}[2(\Gamma+\kappa_1)+n\kappa_1(\Gamma\gamma_1+\gamma_2)]\}}{2(\Gamma+\kappa_1)(\Gamma\kappa_2+1)+(\Gamma\gamma_1+\gamma_2)[n\kappa_1+\Gamma\kappa_2(n-2)+\kappa_1\kappa_2(n-2+n\Gamma)]}, \end{aligned} \tag{39}$$

at $t = 0$. Consequently, it follows from the above and Eq. (38) that

$$\begin{bmatrix} d_1 \\ d_2 \end{bmatrix} = \frac{\Gamma(\kappa_2+1)}{2(\Gamma+\kappa_1)(\Gamma\kappa_2+1)+(\Gamma\gamma_1+\gamma_2)[n\kappa_1+\Gamma\kappa_2(n-2)+\kappa_1\kappa_2(n-2+n\Gamma)]}\boldsymbol{\Omega}_n^{-1} \times \begin{bmatrix} \kappa_1\{E_n[2(\Gamma\kappa_2+1)+\kappa_2(n-2)(\Gamma\gamma_1+\gamma_2)] + \overline{F}_{n-2}(n-2)(\Gamma\gamma_1+\gamma_2)\} \\ E_n n\kappa_1\kappa_2(\Gamma\gamma_1+\gamma_2) + \overline{F}_{n-2}[2(\Gamma+\kappa_1)+n\kappa_1(\Gamma\gamma_1+\gamma_2)] \end{bmatrix}, \tag{40}$$

where the 2 × 2 matrix $\boldsymbol{\Omega}_n$ is defined by

$$\boldsymbol{\Omega}_n = [\mathbf{I}_{2\times2} \quad 0_{2\times2}][\mathbf{v}_n^{+} \quad \mathbf{v}_n^{-}] = [\mathbf{I}_{2\times2} \quad 0_{2\times1}][\mathbf{w}_n^{+} \quad \mathbf{w}_n^{-}]. \tag{41}$$

The inverse of $\boldsymbol{\Omega}_n$ can then be given quite simply by

$$\boldsymbol{\Omega}_n^{-1} = \frac{1}{[\mathbf{w}_n^{+}]_1[\mathbf{w}_n^{-}]_2 - [\mathbf{w}_n^{-}]_1[\mathbf{w}_n^{+}]_2}\begin{bmatrix} [\mathbf{w}_n^{-}]_2 & -[\mathbf{w}_n^{-}]_1 \\ -[\mathbf{w}_n^{+}]_2 & [\mathbf{w}_n^{+}]_1 \end{bmatrix}. \tag{42}$$

The detailed expressions of $[\mathbf{w}_n^{\pm}]_1$ and $[\mathbf{w}_n^{\pm}]_2$ can be found in the Appendix.

It follows from Eqs. (11) and (12) that $\psi_1(z)$ defined in the inhomogeneity and $\psi_2(z)$ defined in the matrix can be given as

It is observed from the above analysis that the two coefficients X_1 and B_1 are time-independent, whereas the remaining coefficients X_m, Y_n, A_n, B_m, $(n, m \geq 0$ and $m \neq 1)$ are time-dependent: X_2, B_2 and $\kappa_1 X_0 + Y_0 - \Gamma(\kappa_2 A_0 + B_0)$ evolve with a single relaxation time t_0; X_n, Y_{n-2}, B_n, A_{n-2}, $(n \geq 3)$ evolve with two relaxation times t_n^{+} and t_n^{-}. Substituting the two pairs of analytic functions $\phi_1(z)$, $\psi_1(z)$, $(|z|<R)$ and $\phi_2(z)$, $\psi_2(z)$, $(|z|>R)$ into Eq. (2), we can further obtain the stress and displacement fields. Clearly, the stress and displacement fields in the composite depend on four size-dependent dimensionless parameters γ_1, δ_1, γ_2, δ_2 and on two size-dependent parameters ρ, χ and evolve with an infinite number of size-dependent relaxation times: t_0, t_n^{+}, t_n^{-}, $n = 3, 4, \cdots, +\infty$. It is verified that when the surface elasticities are absent (by setting $\gamma_1 = \gamma_2 = 0$), the relaxation times in Eqs. (29) and (34) correspond to those found in Wang and Pan (2011). Note that the relaxation times are independent of the residual surface tensions. It is also seen from the above analysis that in the absence of surface elasticity for both the inhomogeneity and the matrix (i.e., $\gamma_1 = \gamma_2 = \delta_1 = \delta_2 = 0$), our solution at the instant $t = 0$ recovers the classical solution of Dundurs and Mura (1964) for a perfectly bonded interface.

The average mean stress within the inhomogeneity and the rigid-body rotation at the centre of the circular inhomogeneity,

both of which are time-independent, can be derived quite simply as

$$<\sigma_{11}+\sigma_{22}> = -\frac{4\mu_1\left[\frac{b_2}{\pi\xi}+2(\Gamma\delta_1+\delta_2)\right]}{2\Gamma+(\kappa_1-1)(1+\Gamma\gamma_1+\gamma_2)}, \tag{44}$$

$$\varpi_{21}=\frac{1}{2}(u_{2,1}-u_{1,2})=\frac{b_1}{2\pi\xi},\ \text{at } z=0, \tag{45}$$

(47), we have assumed that $X_0=Y_0=0$. In the two pairs of analytic functions, the two time-independent coefficients X_1 and B_1 remain as in Eq. (21) and the remaining coefficients are determined by

$$B_2=\frac{E_2(1-\gamma_2\kappa_2)}{1+\gamma_2},\quad \kappa_2A_0+B_0=\frac{\overline{E}_2(\kappa_2+1)(\chi-\rho)}{(1+\gamma_2)(\rho+\chi)}-\kappa_2E_0, \tag{48}$$

$$\begin{bmatrix}\kappa_1X_n\\ \overline{Y}_{n-2}\\ \Gamma B_n\\ \Gamma\kappa_2\overline{A}_{n-2}\end{bmatrix}=d_1\mathbf{v}_3^+e^{-t/t_3^+}\delta_{n3}+\frac{\Gamma}{2+\gamma_2[n+\kappa_2(n-2)]}\begin{bmatrix}0\\0\\2(1-\gamma_2\kappa_2)E_n+\gamma_2(n-2)(1+\kappa_2)\overline{F}_{n-2}\\ n\gamma_2\kappa_2(1+\kappa_2)E_n+2\kappa_2(1+\gamma_2)\overline{F}_{n-2}\end{bmatrix},\ n=3,4,\cdots,+\infty, \tag{49}$$

where <*> denotes the average. It is observed from Eq. (44) that the sign of the average mean stress is simply opposite to that of $[b_2/(\pi\xi)+2(\Gamma\delta_1+\delta_2)]$. The average mean stress inside the inhomogeneity will become zero when $b_2=-2\pi\xi(\Gamma\delta_1+\delta_2)$. Interestingly, the rigid-body rotation at the centre of the inhomogeneity in Eq. (45) is dependent only on b_1 and ξ.

As $t\to\infty$, the internal steady-state stress field inside the inhomogeneity is uniform and hydrostatic and is given by

$$\sigma_{11}=\sigma_{22}=-\frac{2\mu_1\left[\frac{b_2}{\pi\xi}+2(\Gamma\delta_1+\delta_2)\right]}{2\Gamma+(\kappa_1-1)(1+\Gamma\gamma_1+\gamma_2)},\qquad \sigma_{12}=0,\quad z\in S_1 \text{ and } t\to\infty. \tag{46}$$

Our numerical results indicate that t_3^+ is the longest relaxation time among all of the relaxation times $t_0,\ t_n^+,\ t_n^-,\ n=3,4,\cdots,+\infty$ for finite and nonzero values of ρ and χ. Consequently for the long range stress relaxations, the two analytic functions defined in the inhomogeneity can be written approximately in the following closed-form

where d_1 is determined by Eq. (40) with $n=3$.

The internal stress field determined by Eq. (47) is a quadratic function of the coordinates x_1 and x_2 and decays with the longest relaxation time t_3^+.

4. Image force on the edge dislocation

The image force acting on the edge dislocation can be conveniently obtained by using the solution derived in the previous section and the Peach-Koehler formula (Dundurs, 1969). In this section, we will present explicit expressions for the image force for two typical cases: (i) the dislocation contains only the gliding component with $b_1\neq0$ and $b_2=0$; (ii) the dislocation contains only the climbing component with $b_2\neq0$ and $b_1=0$.

4.1. $b_1\neq0,\ b_2=0$

The image force acting on the gliding dislocation can be derived as

$$\begin{aligned}F^*&=\frac{\pi R(\kappa_2+1)}{\mu_2b_1^2}F_1=\frac{1}{1+\gamma_2}\left[\frac{\Gamma(\kappa_2+1)(1+\kappa_1\gamma_1)}{\Gamma+\kappa_1(1+\Gamma\gamma_1+\gamma_2)}e^{-t/t_0}-1+\gamma_2\kappa_2\right]\eta^5\\ &+2\left(1-\eta^2\right)\left[(1-\gamma_2\kappa_2)\eta^2-(1+\gamma_2)\right]\sum_{n=3}^{+\infty}\frac{\eta^{2n-3}(n-1)^2}{2+\gamma_2[n+\kappa_2(n-2)]}\\ &+(\kappa_2+1)\sum_{n=3}^{+\infty}\frac{\eta^{2n-3}}{n(n-2)\{2(\Gamma+\kappa_1)(\Gamma\kappa_2+1)+(\Gamma\gamma_1+\gamma_2)[n\kappa_1+\Gamma\kappa_2(n-2)+\kappa_1\kappa_2(n-2+n\Gamma)]\}}\\ &\times\left[0,\quad 0,\quad n\eta^2,\quad \kappa_2^{-1}(n-2)\left(n-1-n\eta^2\right)\right]\left[e^{-t/t_n^+}\mathbf{v}_n^+,\quad e^{-t/t_n^-}\mathbf{v}_n^-\right]\mathbf{\Omega}_n^{-1}\\ &\times\begin{bmatrix}\kappa_1(n-2)\left\{\eta^2[-2(\Gamma\kappa_2+1)+(n-2)(n-\kappa_2)(\Gamma\gamma_1+\gamma_2)]-n(n-1)(\Gamma\gamma_1+\gamma_2)\right\},\\ \eta^2n(n-2)[2(\Gamma+\kappa_1)+\kappa_1(n-\kappa_2)(\Gamma\gamma_1+\gamma_2)]-n(n-1)[2(\Gamma+\kappa_1)+n\kappa_1(\Gamma\gamma_1+\gamma_2)]\end{bmatrix},\end{aligned} \tag{50}$$

$$\begin{aligned}\varphi_1(z)&\approx X_1R^{-1}z+X_3R^{-3}z^3,\\ \psi_1(z)&\approx-\left(\overline{Y}_1+3X_3\right)R^{-1}z,\quad |z|<R,\end{aligned} \tag{47}$$

whilst the two analytic functions $\phi_2(z),\ \psi_2(z),\ |z|>R$ are still given by the series form expressions in Eq. $(12)_2$ and $(43)_2$. In writing Eq.

where F_1 is the image force component along the x_1 direction, and $\eta=R/\xi,\ -1<\eta<1$ is the introduced dislocation location parameter. It is observed from Eq. (50) that: (i) the normalized image force F^* is reliant on the two size-dependent parameters $\gamma_1,\ \gamma_2$ and evolves with an infinite number of relaxation times $t_0,\ t_n^+,\ t_n^-,\ n=3,4,\cdots,+\infty$; (ii) F^* is an odd function of η. We illustrate in Fig. 2 the normalized image force on a gliding

dislocation at different instances with $\Gamma=3$, $\kappa_1=\kappa_2=2$, $\gamma_1=0.1$, $\gamma_2=0.3$ and $\rho=\chi$. The results for $t=0$ and $t=\infty$ in Fig. 2 are consistent with our recent study on a mixed-type imperfect interface which is composed of a spring-type interface lying between two stiff interfaces arising from surface elasticities (Wang and Schiavone, 2016). It is clearly observed from Fig. 2 that there exists a transient unstable equilibrium position when $t=0.001\rho,\ 0.01\rho,\ 0.1\rho$. This transient equilibrium position moves away from the inhomogeneity as time increases. Also observed from our numerical results for the same set of material parameters (which are not shown in Fig. 2) is the co-existence of another transient stable equilibrium position extremely close to the inhomogeneity-matrix interface (i.e., $\eta\approx 1$) for $t>0$ resulting from the surface elasticity for the matrix.

The asymptotic expression of the image force when the gliding dislocation is very far from the inhomogeneity can be extracted from Eq. (50) as

$$F^*\cong -\eta^3\left(\begin{array}{l}\dfrac{8(1+\gamma_2)}{2+\gamma_2(3+\kappa_2)}+\dfrac{4(\kappa_2+1)}{\kappa_2\{2(\Gamma+\kappa_1)(\Gamma\kappa_2+1)+(\Gamma\gamma_1+\gamma_2)[3\kappa_1+\Gamma\kappa_2+\kappa_1\kappa_2(1+3\Gamma)]\}}\\ \times\left[\mathrm{e}^{-t/t_3^+}\quad \mathrm{e}^{-t/t_3^-}\right]\boldsymbol{\Omega}_3^{-1}\left[\begin{array}{c}\kappa_1(\Gamma\gamma_1+\gamma_2)\\ 2(\Gamma+\kappa_1)+3\kappa_1(\Gamma\gamma_1+\gamma_2)\end{array}\right]\end{array}\right)+O\left(\eta^5\right),\ \eta\to 0. \tag{51}$$

In deriving the above expression, the last components of $\mathbf{v}_3^+$ and $\mathbf{v}_3^-$ have been set to be 1, as in Eq. (36). The asymptotic expression in Eq. (51) evolves with two relaxation times t_3^+ and t_3^-.

4.2. $b_2\neq 0,\ b_1=0$

The image force acting on the climbing dislocation is given explicitly by

$$\begin{aligned}F_*&=\frac{\pi R(\kappa_2+1)}{\mu_2 b_2^2}F_1=-\frac{R}{b_2}\frac{2\pi(\kappa_1-1)(\kappa_2+1)(\Gamma\delta_1+\delta_2)}{2\Gamma+(\kappa_1-1)(1+\Gamma\gamma_1+\gamma_2)}\eta^2\\&+\frac{2\Gamma(\kappa_2-1)-2(\kappa_1-1)+(\kappa_1-1)(\kappa_2-1)(\Gamma\gamma_1+\gamma_2)}{2\Gamma+(\kappa_1-1)(1+\Gamma\gamma_1+\gamma_2)}\eta^3\\&+\frac{1}{1+\gamma_2}\left[\frac{\Gamma(\kappa_2+1)(1+\kappa_1\gamma_1)}{\Gamma+\kappa_1(1+\Gamma\gamma_1+\gamma_2)}\mathrm{e}^{-t/t_0}-(1-\gamma_2\kappa_2)\right]\eta^5\\&+2\sum_{n=3}^{+\infty}\eta^{2n-3}\frac{\left[\eta^2(n-1)-(n-3)\right]\left[\eta^2(n-1)(\gamma_2\kappa_2-1)+(n-3)(1+\gamma_2)\right]}{2+\gamma_2[n+\kappa_2(n-2)]}\\&+(\kappa_2+1)\sum_{n=3}^{+\infty}\frac{\eta^{2n-3}}{n(n-2)\{2(\Gamma+\kappa_1)(\Gamma\kappa_2+1)+(\Gamma\gamma_1+\gamma_2)[n\kappa_1+\Gamma\kappa_2(n-2)+\kappa_1\kappa_2(n-2+n\Gamma)]\}}\\&\times\left[0,\quad 0,\quad n\eta^2,\quad \kappa_2^{-1}(n-2)\left(n-3-n\eta^2\right)\right]\left[\mathbf{v}_n^+\mathrm{e}^{-t/t_n^+},\quad \mathbf{v}_n^-\mathrm{e}^{-t/t_n^-}\right]\boldsymbol{\Omega}_n^{-1}\\&\times\left[\begin{array}{l}\kappa_1(n-2)\left\{\eta^2[-2(\Gamma\kappa_2+1)+(n-2)(n-\kappa_2)(\Gamma\gamma_1+\gamma_2)]-n(n-3)(\Gamma\gamma_1+\gamma_2)\right\},\\ n(n-2)[2(\Gamma+\kappa_1)+\kappa_1(n-\kappa_2)(\Gamma\gamma_1+\gamma_2)]\eta^2-n(n-3)[2(\Gamma+\kappa_1)+n\kappa_1(\Gamma\gamma_1+\gamma_2)]\end{array}\right].\end{aligned} \tag{52}$$

It is observed from Eq. (52) that: (i) the normalized image force F_* depends on the five size-dependent parameters $\gamma_1,\ \delta_1,\ \gamma_2,\ \delta_2$ and R/b_2 and evolves with an infinite number of size-dependent relaxation times: $t_0,\ t_n^+,\ t_n^-,\ n=3,\ 4,\cdots,+\infty$; (ii) F_* is no longer an odd function of η due to the existence of the residual surface tensions. We illustrate in Fig. 3 the normalized image force on a climbing dislocation at different instances with $\Gamma=3$, $\kappa_1=\kappa_2=2$, $\gamma_1=0.1$, $\gamma_2=0.2$, $\delta_1=\delta_2=0$ and $\rho=\chi$. The curve for $t=0$ in Fig. 3 indeed recovers our recent result for a mixed-type imperfect interface (Wang and Schiavone, 2016). However, the curve for $t=\infty$ in Fig. 3 cannot be directly obtained from the result of a mixed-type interface mainly because of the presence of the hydrostatic normal stress acting on the boundary of the matrix as time approaches infinity. It is observed from Fig. 3 that the dislocation is repelled from the inhomogeneity when $t<3.321\rho$; a transient stable and another transient unstable equilibrium positions co-exist when $t>3.321\rho$.

The asymptotic expression of the image force when the climbing dislocation is very far from the inhomogeneity can be extracted from Eq. (52) as

$$\begin{aligned}F_*=&-\frac{R}{b_2}\frac{2\pi(\kappa_1-1)(\kappa_2+1)(\Gamma\delta_1+\delta_2)}{2\Gamma+(\kappa_1-1)(1+\Gamma\gamma_1+\gamma_2)}\eta^2\\&+\frac{2\Gamma(\kappa_2-1)-2(\kappa_1-1)+(\kappa_1-1)(\kappa_2-1)(\Gamma\gamma_1+\gamma_2)}{2\Gamma+(\kappa_1-1)(1+\Gamma\gamma_1+\gamma_2)}\eta^3\\&+O\left(\eta^5\right),\ \eta\to 0.\end{aligned} \tag{53}$$

Interestingly, interface slip and diffusion exert no influence on the above time-independent asymptotic expression. As $\eta\to 0$, the sign of F_* is simply opposite to that of b_2.

5. Discussion of the relaxation times

It is found from the analysis in Sections 3 and 4 that the evolution of the elastic field in the composite and that of the image force are determined by the relaxation times $t_0,\ t_n^+,\ t_n^-,\ n=3,\ 4,\cdots,+\infty$. In this section, with our primary goal to demonstrate the solution, the values of these relaxation times will be presented specifically for five special cases: (i) the interface diffusion is absent ($\rho\to\infty$); (ii) the interface slip is absent ($\chi\to\infty$); (iii) the interface diffusion occurs much faster than the interface slip ($\rho=0$); (iv) the interface slip occurs much faster than the interface diffusion ($\chi=0$); (v) $\gamma_1,\gamma_2\to\infty$.

5.1. $\rho\to\infty$

In this case, it follows from Eqs. (29), (34) and (35) that

$$\begin{aligned}
&\frac{t_0}{\chi}=\frac{\Gamma+\kappa_1(1+\Gamma\gamma_1+\gamma_2)}{(1+\kappa_1\gamma_1)(1+\gamma_2)},\\
&\frac{t_n^-}{\chi}=\frac{4(\Gamma+\kappa_1)(\Gamma\kappa_2+1)+2(\Gamma\gamma_1+\gamma_2)[n\kappa_1(\Gamma\kappa_2+1)+\kappa_2(n-2)(\Gamma+\kappa_1)]}{2(n-2)(\Gamma+\kappa_1)+2n(\Gamma\kappa_2+1)},\\
&\left(\begin{array}{l}
+\gamma_1\left\{\Gamma(n-2)^2+\kappa_1\left[4(n-1)^2+\Gamma n(n-2)\right]+\Gamma\kappa_2 n(n-2)+\Gamma\kappa_1\kappa_2 n^2\right\}\\
+\gamma_2\left\{n^2+\kappa_1 n(n-2)+\kappa_2\left[n(n-2)+4\Gamma(n-1)^2\right]+\kappa_1\kappa_2(n-2)^2\right\}\\
+2\gamma_1\gamma_2(n-1)^2[n\kappa_1+\Gamma\kappa_2(n-2)+\kappa_1\kappa_2(\Gamma n+n-2)]
\end{array}\right)\\
&t_n^+\to\infty.
\end{aligned}\tag{54}$$

5.2. $\chi\to\infty$

In this case, from Eqs. (29), (34) and (35), we find that

$$\begin{aligned}
&\frac{t_0}{\rho}=\frac{\Gamma+\kappa_1(1+\Gamma\gamma_1+\gamma_2)}{(1+\kappa_1\gamma_1)(1+\gamma_2)},\\
&\frac{t_n^-}{\rho}=\frac{4(\Gamma+\kappa_1)(\Gamma\kappa_2+1)+2(\Gamma\gamma_1+\gamma_2)[n\kappa_1(\Gamma\kappa_2+1)+\kappa_2(n-2)(\Gamma+\kappa_1)]}{2(n-2)(\Gamma+\kappa_1)+2n(\Gamma\kappa_2+1)},\\
&(n-1)^2\left(\begin{array}{l}
+\gamma_1\left[\Gamma(n-2)^2+\kappa_1[4+\Gamma n(n-2)]+\Gamma\kappa_2 n(n-2)+\Gamma\kappa_1\kappa_2 n^2\right]\\
+\gamma_2\left[n^2+\kappa_1 n(n-2)+\kappa_2[n(n-2)+4\Gamma]+\kappa_1\kappa_2(n-2)^2\right]\\
+2\gamma_1\gamma_2[n\kappa_1+\Gamma\kappa_2(n-2)+\kappa_1\kappa_2(n-2+n\Gamma)]
\end{array}\right)\\
&t_n^+\to\infty.
\end{aligned}\tag{55}$$

5.3. $\rho=0$

Here, from Eqs. (29), (34) and (35) we have

$$t_0=t_n^-=0,\quad \frac{t_n^+}{\chi}=\frac{\left(\begin{array}{l}
2(n-2)(\Gamma+\kappa_1)+2n(\Gamma\kappa_2+1)\\
+\gamma_1\left[\Gamma(n-2)^2+\kappa_1[4+\Gamma n(n-2)]+\Gamma\kappa_2 n(n-2)+\Gamma\kappa_1\kappa_2 n^2\right]\\
+\gamma_2\left[n^2+\kappa_1 n(n-2)+\kappa_2[n(n-2)+4\Gamma]+\kappa_1\kappa_2(n-2)^2\right]\\
+2\gamma_1\gamma_2[n\kappa_1+\Gamma\kappa_2(n-2)+\kappa_1\kappa_2(n-2+n\Gamma)]
\end{array}\right)}{n(n-2)[2+\gamma_1(n\kappa_1+n-2)][2+\gamma_2[n+\kappa_2(n-2)]]}.\tag{56}$$

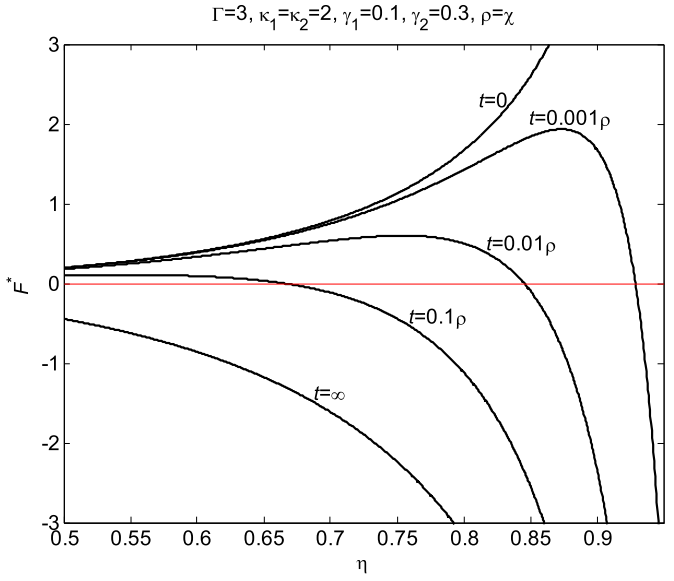

Fig. 2. The normalized image force F^* on a gliding dislocation at five moments $t = 0,\ 0.001\rho,\ 0.01\rho,\ 0.1\rho,\ \infty$ with $\Gamma = 3,\ \kappa_1 = \kappa_2 = 2,\ \gamma_1 = 0.1,\ \gamma_2 = 0.3$ and $\rho = \chi$.

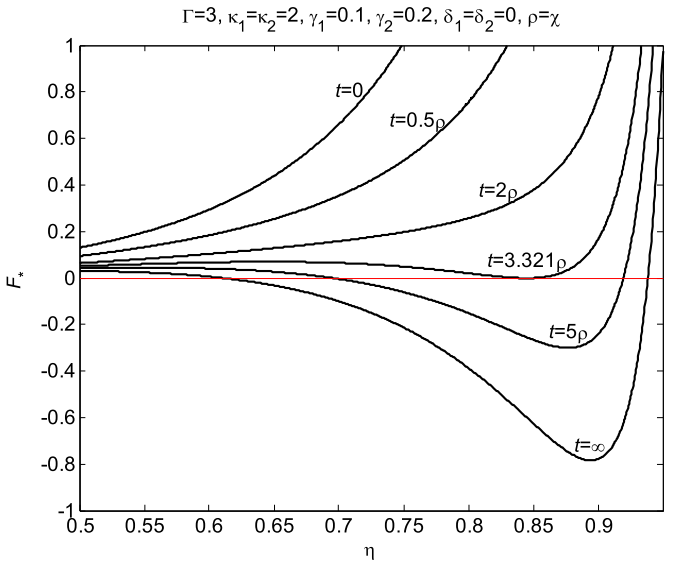

Fig. 3. The normalized image force F_* on a climbing dislocation at six moments $t = 0,\ 0.5\rho,\ 2\rho,\ 3.321\rho,\ 5\rho,\ \infty$ with $\Gamma = 3,\ \kappa_1 = \kappa_2 = 2,\ \gamma_1 = 0.1,\ \gamma_2 = 0.2,\ \delta_1 = \delta_2 = 0$ and $\rho = \chi$.

5.4. $\chi = 0$

From Eqs. (29), (34) and (35), we find that

$$t_0 = t_n^- = 0, \quad \frac{t_n^+}{\rho} = \frac{\begin{pmatrix} 2(n-2)(\Gamma+\kappa_1) + 2n(\Gamma\kappa_2+1) \\ +\gamma_1\left\{\Gamma(n-2)^2 + \kappa_1\left[4(n-1)^2 + \Gamma n(n-2)\right] + \Gamma\kappa_2 n(n-2) + \Gamma\kappa_1\kappa_2 n^2\right\} \\ +\gamma_2\left\{n^2 + \kappa_1 n(n-2) + \kappa_2\left[n(n-2) + 4\Gamma(n-1)^2\right] + \kappa_1\kappa_2(n-2)^2\right\} \\ +2\gamma_1\gamma_2(n-1)^2[n\kappa_1 + \Gamma\kappa_2(n-2) + \kappa_1\kappa_2(\Gamma n + n - 2)] \end{pmatrix}}{n(n-1)^2(n-2)[2+\gamma_1(n\kappa_1+n-2)][2+\gamma_2[n+\kappa_2(n-2)]]}. \tag{57}$$

5.5. $\gamma_1, \gamma_2 \to \infty$

Finally, it follows from Eqs. (29), (34) and (35) that

$$t_0 = t_n^- = 0, \quad t_n^+ = \frac{2(\rho+\chi)[n\kappa_1 + \Gamma\kappa_2(n-2) + \kappa_1\kappa_2(\Gamma n + n - 2)]}{n(n-2)(n\kappa_1 + n - 2)[n + \kappa_2(n-2)]}. \tag{58}$$

6. Conclusions

We have rigorously derived an analytical solution in series-form to the interaction problem associated with an edge dislocation near a nanosized circular elastic inhomogeneity with interface slip and diffusion. Firstly, the two analytic functions $\phi_1(z),\ \phi_2(z)$ and their analytical continuations are decomposed into Eq. (14). In doing so, the need to use the second-order tangential derivative with respect to interface normal traction can be circumvented. When choosing $\phi_1(z) = \phi_1^{(1)}(z)$ and $\phi_2(z) = \phi_2^{(1)}(z)$, the solution is independent of time and we arrive at two coupled linear algebraic equations for X_1 and B_1. When choosing $\phi_1(z) = \phi_1^{(2)}(z)$ and $\phi_2(z) = \phi_2^{(2)}(z)$, a state-space representation for $X_2,\ B_2$ and $\kappa_1 X_0 + Y_0 - \Gamma(\kappa_2 A_0 + B_0)$, which contains only a single relaxation time t_0, is obtained in Eq. (26). When choosing $\phi_1(z) = \phi_1^{(n)}(z)$ and $\phi_2(z) = \phi_2^{(n)}(z)$ with $n \geq 3$, mutually independent sets of state-space equations for $X_n,\ Y_{n-2}, B_n,\ A_{n-2}$ are derived in Eq. (30) which contains two relaxation times t_n^+ and t_n^-. All the relaxation times of the composite are given explicitly in Eqs. (29) and (34).

Our analysis indicates that the induced elastic fields describing stresses and displacements in the composite and the normalized image force acting on the edge dislocation depend on the four size-dependent dimensionless parameters $\gamma_1,\ \gamma_2,\ \delta_1,\ \delta_2$ and on two size-dependent parameters $\rho,\ \chi$ having the dimension of time and evolve with an infinite number of size-dependent relaxation times: $t_0,\ t_n^+,\ t_n^-,\ n = 3,\ 4, \cdots, +\infty$. In addition F_* in Eq. (52) on a climbing dislocation is no longer an odd function of η and is also dependent on another size-dependent parameter R/b_2 as a result of the presence of residual surface tensions. Interestingly, both the average mean stress within the circular inhomogeneity in Eq. (44) and the rigid-body rotation at the centre of the inhomogeneity in Eq. (45) are time-independent. The steady-state internal stress field inside the inhomogeneity induced by the edge dislocation is uniform and hydrostatic.

Acknowledgements

We are grateful to a reviewer for his/her very helpful comments and suggestions. This work is supported by the National Natural Science Foundation of China (Grant No: 11272121) and through a Discovery Grant from the Natural Sciences and Engineering Research Council of Canada (Grant # RGPIN 155112).

Appendix

The three components of $\mathbf{w}_n^{\pm}$ are explicitly given by

$$
\begin{aligned}
[\mathbf{w}_n^{\pm}]_1 &= \frac{2\kappa_1(n-2)\{\rho_n t_n^{\pm}[1+\gamma_1(n-1)][1+\gamma_2(n-1)] - \chi t_n^{\pm}(1-\gamma_1)(1+\gamma_2) - \rho_n\chi(\Gamma\gamma_1+\gamma_2)\}}{\Delta},\\
[\mathbf{w}_n^{\pm}]_2 &= \frac{2\{n\rho_n t_n^{\pm}[1+\gamma_1\kappa_1(n-1)][1+\gamma_2(n-1)] + n\chi t_n^{\pm}(1+\gamma_1\kappa_1)(1+\gamma_2) - \rho_n\chi[2(\Gamma+\kappa_1)+n\kappa_1(\Gamma\gamma_1+\gamma_2)]\}}{\Delta},\\
[\mathbf{w}_n^{\pm}]_3 &= \frac{(n-2)\begin{pmatrix}\rho_n(t_n^{\pm})\left[-2\Gamma-\Gamma\gamma_1(n-2+n\kappa_1)+\gamma_2[n+\kappa_1(n-2)]+2\gamma_1\gamma_2\kappa_1(n-1)^2\right]\\ +\chi(t_n^{\pm})[2\Gamma+\Gamma\gamma_1(n-2+n\kappa_1)+\gamma_2[n+\kappa_1(n-2)]+2\gamma_1\gamma_2\kappa_1]\\ -2\rho_n\chi\kappa_1(\Gamma\gamma_1+\gamma_2)-(t_n^{\pm})^2 n(n-2)[2\gamma_2+\gamma_1\gamma_2(n-2+n\kappa_1)]\end{pmatrix}}{\Delta},
\end{aligned}
\tag{A1}
$$

where

$$
\begin{aligned}
\Delta = {}& \rho_n t_n^{\pm}\begin{pmatrix}2n+2(\Gamma+\kappa_1)(n-2)+\gamma_1\left[4\kappa_1(n-1)^2+\Gamma\kappa_1 n(n-2)+\Gamma(n-2)^2\right]\\ +n\gamma_2[n+\kappa_1(n-2)]+2n\gamma_1\gamma_2\kappa_1(n-1)^2\end{pmatrix}\\
&+\chi t_n^{\pm}\begin{pmatrix}2n+2(\Gamma+\kappa_1)(n-2)+\gamma_1\left[4\kappa_1+\Gamma\kappa_1 n(n-2)+\Gamma(n-2)^2\right]\\ +n\gamma_2[n+\kappa_1(n-2)]+2n\gamma_1\gamma_2\kappa_1\end{pmatrix}\\
&-2\rho_n\chi[2(\Gamma+\kappa_1)+n\kappa_1(\Gamma\gamma_1+\gamma_2)]-(t_n^{\pm})^2 n(n-2)(2+\gamma_2 n)[2+\gamma_1(\kappa_1 n+n-2)].
\end{aligned}
\tag{A2}
$$

The correctness of Eq. (A1) has been numerically verified.

References

Antipov, Y.A., Schiavone, P., 2011. Integro-differential equation for a finite crack in a strip with surface effects. Q. J. Mech. Appl. Math. 64, 87–106.

Chen, T., Dvorak, G.J., Yu, C.C., 2007. Size-dependent elastic properties of unidirectional nano-composites with interface stresses. Acta Mech. 188, 39–54.

Dundurs, J., 1969. In: Mura, T. (Ed.), Elastic Interaction of Dislocations with Inhomogeneities. Mathematical Theory of Dislocations. American Society of Mechanical Engineers, New York, pp. 70–115.

Dundurs, J., Mura, T., 1964. Interaction between an edge dislocation and a circular inclusion. J. Mech. Phys. Solids 12, 177–189.

Gurtin, M.E., Murdoch, A., 1975. A continuum theory of elastic material surfaces. Arch. Ration. Mech. Anal 57, 291–323.

Gurtin, M.E., Murdoch, A.I., 1978. Surface stress in solids. Int. J. Solids Struct. 14, 431–440.

Gurtin, M.E., Weissmuller, J., Larche, F., 1998. A general theory of curved deformable interface in solids at equilibrium. Philos. Mag. A 78, 1093–1109.

Herring, C., 1950. Diffusional viscosity of a polycrystalline solid. J. Appl. Phys. 21, 437–445.

Kim, K.T., McMeeking, R.M., 1995. Power law creep with interface slip and diffusion in a composite material. Mech. Mater. 20, 153–164.

Koeller, R.C., Raj, R., 1978. Diffusional relaxation on stress concentration at second-phase particles. Acta Metall. 26, 1551–1558.

Markenscoff, X., Dundurs, J., 2014. Annular inhomogeneities with eigenstrain and interphase modeling. J. Mech. Phys. Solids 64, 468–482.

Muskhelishvili, N.I., 1953. Some Basic Problems of the Mathematical Theory of Elasticity. P. Noordhoff Ltd, Groningen.

Onaka, S., Huang, J.H., Wakashima, K., Mori, T., 1998. Kinetics of stress relaxation caused by the combination of interfacial sliding and diffusion: two-dimensional analysis. Acta Mater. 46, 3821–3828.

Raj, R., Ashby, M.F., 1971. On grain boundary sliding and diffusional creep. Metall. Trans. 2, 1113–1127.

Ru, C.Q., 2010. Simple geometrical explanation of Gurtin-Murdoch model of surface elasticity with clarification of its related versions. Sci. China 53, 536–544.

Sharma, P., Ganti, S., 2004. Size-dependent Eshelby's tensor for embedded nano-inclusions incorporating surface/interface energies. ASME J. Appl. Mech. 71, 663–671.

Sofronis, P., McMeeking, R.M., 1994. The effect of interface diffusion and slip on the creep resistance of particulate composite materials. Mech. Mater. 18, 55–68.

Srolovitz, D.J., Luton, M.J., Petkovic-Luton, R., Barnett, D.M., Nix, W.D., 1984. Diffusionally modified dislocation-particle elastic interactions. Acta Metall. 32, 1079–1088.

Steigmann, D.J., Ogden, R.W., 1997. Plane deformations of elastic solids with intrinsic boundary elasticity. Proc. R. Soc. Lond. A 453, 853–877.

Ting, T.C.T., 1996. Anisotropic Elasticity-theory and Applications. Oxford University Press, New York.

Wang, X., Pan, E., 2010. A circular inhomogeneity with interface slip and diffusion under in-plane deformation. Int. J. Eng. Sci. 48, 1733–1748.

Wang, X., Pan, E., 2011. Interaction between an edge dislocation and a circular inclusion with interface slip and diffusion. Acta Mater. 59, 797–804.

Wang, X., Schiavone, P., 2016. Interaction between an edge dislocation and a circular inhomogeneity with a mixed-type imperfect interface. Arch. Appl. Mech. (in press).

Wang, X., Wang, C.Y., Schiavone, P., 2016. In-plane deformations of a nano-sized circular inhomogeneity with interface slip and diffusion. Int. J. Eng. Sci. 108, 9–15.

Wei, Y.J., Bower, A.F., Gao, H.J., 2008. Recoverable creep deformation and transient local stress concentration due to heteregeneous grain-boundary diffusion and sliding in polycrystalline solids. J. Mech. Phys. Solids 56, 1460–1483.